IMA Journal of Applied Mathematics (2018) Page 1 of 19
doi:10.1093/imamat/drnxxx

The electromagnetic scattering problem by a cylindrical doubly-connected domain at oblique incidence: the direct problem

LEONIDAS MINDRINOS
Faculty of Mathematics, University of Vienna,
Oskar-Morgenstern-Platz 1, 1090 Vienna, Austria
leonidas.mindrinos@univie.ac.at

[Received on 10 October 2018]

We consider the direct electromagnetic scattering problem of time-harmonic obliquely incident waves by a infinitely long, homogeneous and doubly-connected cylinder in three dimensions. We apply a hybrid integral equation method (combination of the direct and indirect methods) and we transform the scattering problem to a system of singular and hypersingular integral equations. The well-posedness of the corresponding problem is proven. We use trigonometric polynomial approximations and we solve the system of the discretized integral operators by a collocation method.

Keywords: direct electromagnetic scattering, oblique incidence, integral equation method, trigonometric quadrature rules, collocation method

1. Introduction

The scattering problem of electromagnetic waves by a penetrable medium generates theoretical and numerical questions. Even if it is the direct (given the medium, compute the scattered wave) or the inverse (recover the medium from the far-field pattern) problem, the main and first question to ask is that of the unique solvability. Numerically, both problems can be solved using similar techniques but the nonlinearity and the ill-posedness of the inverse problem have to be taken into account. For a review on scattering theory for solving direct and inverse problems, we refer to the books by Cakoni & Colton (2006); Colton & Kress (2013a,b); Kirsch & Hettlich (2015).

Since we use electromagnetic waves as incident fields the mathematical model is based on Maxwell's equations and the transmission conditions describe the continuity of the tangential components of the electric and magnetic fields. The three-dimensional problem can, however, be reduced to simpler problems for the Helmholtz equation given some assumptions on the incident illumination and the optical properties of the medium.

We specify the medium to be a infinitely long, penetrable cylinder embedded in a homogeneous dielectric medium. The incoming electromagnetic wave is a time-harmonic plane wave at oblique incidence (transverse magnetic polarized). This problem has been considered by many researchers from different fields because of its applications in industry and medical imaging, (see, e.g., Erturk & Rojas, 2000; Lucido et al., 2010; Rojas, 1988; Sarabandi & Senior, 1990). From a mathematical point of view, this scattering problem has also attracted considerable attention. Many methods have been considered for the numerical solution of this problem, (see, e.g., Cangellaris & Lee, 1991; Tsalamengas, 2007; Tsitsas et al., 2007; Wu & Lu, 2008), but only recently the well-posedness of the direct problem has been addressed (see Gintides & Mindrinos (2016); Nakamura & Wang (2013); Wang & Nakamura (2012)).

In this work we extend the results of Gintides & Mindrinos (2016) to the case of a doubly-connected

cylinder. The interior simply connected domain is a perfect electric conductor. This setup is motivated by the analysis of the behavior of antennas and tubes. We consider the Leontovich impedance boundary condition on the inner boundary together with transmission conditions on the outer boundary. Following the work of Wang & Nakamura (2012), we see that the three-dimensional scattering problem is reduced to a system of four two-dimensional Helmholtz equations for the interior and the exterior electric and magnetic fields. The complication of the problem lies in the reformulated boundary conditions where the tangential derivatives of the fields appear.

We consider a hybrid integral equation method, introduced by Kleinman & Martin (1988), meaning a combination of the direct (Green's formulas) and the indirect (single-layer ansatz) methods. The method of boundary integral equations has been considered for solving both direct and inverse scattering problems in different regimes. For some recent applications we refer to the works of Boubendir et al. (2016); Cakoni & Kress (2012); Chapko et al. (2013, 2017); Gintides & Mindrinos (2017); Ivanyshyn & Louër (2016); Wang & Nakamura (2012). We transform the direct problem to a system of singular and hypersingular integral equations. This system is of Fredholm type (uniqueness of solution) and the Fredholm alternative theorem gives existence. We use the collocation method to solve numerically the system of integral equations and we consider the Maue's formula for reducing the hypersingularity of the normal derivative of the double-layer potential (see Kress (1995, 2014a)).

The paper is organized as follows: In Section 2 we formulate the direct scattering problem and we gather the necessary equations and boundary conditions. The existence and uniqueness of solutions, using Green's formulas and the integral equation method, are proved in Section 3. In the last section we present numerical examples with analytic solutions that justify the applicability of the proposed scheme.

2. Formulation of the problem

In this work we consider the scattering of a time-harmonic electromagnetic wave by an infinitely long, penetrable and doubly-connected cylinder in three dimensions. We assume that the cylinder $\Omega_{int} \subset \mathbb{R}^3$ is oriented parallel to the $z-$axis and that it is homogeneous, meaning its properties are described by the constant electric permittivity ε_1 and the magnetic permeability μ_1. The exterior domain $\Omega_{ext} := \mathbb{R}^3 \setminus \overline{\Omega}_{int}$ is characterized equivalently by the constant coefficients ε_0 and μ_0. The smooth boundary $\partial\Omega$ of the cylinder consists of two disjoint surfaces $\partial\Omega_1$ and $\partial\Omega_0$ such that $\partial\Omega = \partial\Omega_1 \cup \partial\Omega_0$, and $\partial\Omega_1 \cap \partial\Omega_0 = \emptyset$. We assume that $\partial\Omega_1$ is contained in the interior of $\partial\Omega_0$.

We define the exterior electric and magnetic fields $\mathbf{E}^{ext}, \mathbf{H}^{ext} : \Omega_{ext} \to \mathbb{C}^3$, respectively and the interior fields $\mathbf{E}^{int}, \mathbf{H}^{int} : \Omega_{int} \to \mathbb{C}^3$, which satisfy the system of Maxwell's equations

$$\begin{aligned} \nabla \times \mathbf{E}^{ext} - i\omega\mu_0 \mathbf{H}^{ext} = 0, \quad \nabla \times \mathbf{H}^{ext} + i\omega\varepsilon_0 \mathbf{E}^{ext} = 0, \quad \text{in } \Omega_{ext}, \\ \nabla \times \mathbf{E}^{int} - i\omega\mu_1 \mathbf{H}^{int} = 0, \quad \nabla \times \mathbf{H}^{int} + i\omega\varepsilon_1 \mathbf{E}^{int} = 0, \quad \text{in } \Omega_{int}, \end{aligned} \tag{2.1}$$

where $\omega > 0$ is the frequency. We impose transmission conditions on the outer boundary

$$\mathbf{n} \times \mathbf{E}^{int} = \mathbf{n} \times \mathbf{E}^{ext}, \quad \mathbf{n} \times \mathbf{H}^{int} = \mathbf{n} \times \mathbf{H}^{ext}, \quad \text{on } \partial\Omega_0, \tag{2.2}$$

and the Leontovich impedance boundary condition on the inner boundary

$$(\mathbf{n} \times \mathbf{E}^{int}) \times \mathbf{n} = \lambda\, \mathbf{n} \times \mathbf{H}^{int}, \quad \text{on } \partial\Omega_1. \tag{2.3}$$

Here $\mathbf{n}$ is the normal vector and $\lambda \in C^1(\partial\Omega_1)$ is the impedance function, assumed to be positive and bounded away from zero. These conditions model a penetrable cylinder which does not allow the fields to penetrate deep into the "hole", the simply-connected domain $\mathbb{R}^3 \setminus (\overline{\Omega}_{int} \cup \overline{\Omega}_{ext})$.

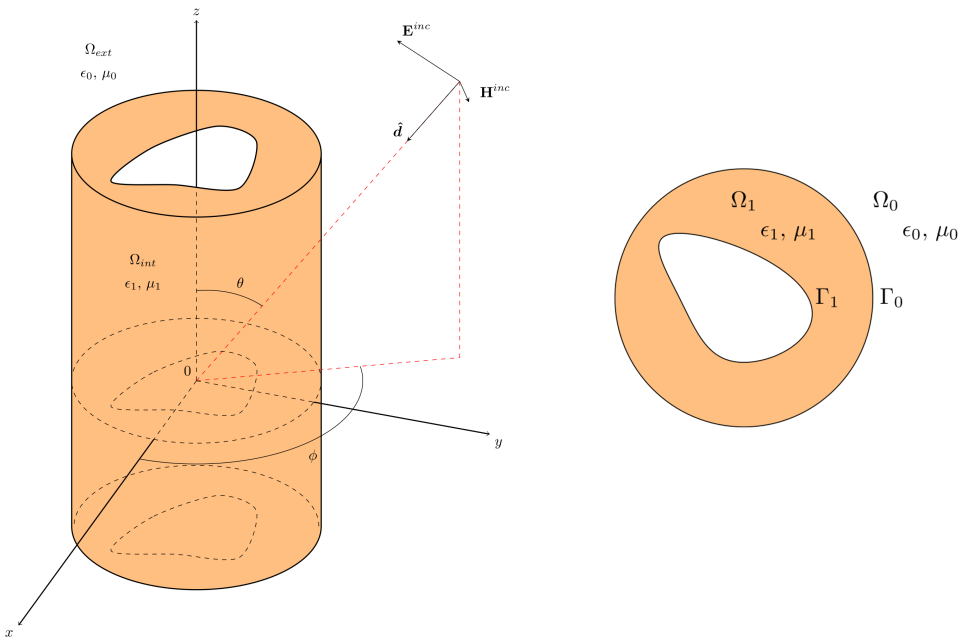

FIG. 1. The geometry of the electromagnetic scattering problem in $\mathbb{R}^3$ for a doubly-connected cylinder oriented parallel to the $z-$axis (left). The horizontal cross section at the plane $z=0$ and the notation used in the two-dimensional problem (right).

The scatterer is illuminated by a time-harmonic transverse magnetic polarized electromagnetic plane wave, the so-called oblique incident wave. The cylindrical symmetry and the homogeneity of the medium reduces the three-dimensional scattering problem (2.1) – (2.3) to a two-dimensional problem only for the $z-$components of the fields, (see, e.g., Gintides & Mindrinos, 2016; Nakamura & Wang, 2013; Wang & Nakamura, 2012).

We define by $\theta \in (0,\pi)$ the incident angle with respect to the negative $z-$axis and by $\phi \in [0,2\pi]$ the polar angle of the incident direction $\hat{\boldsymbol{d}}$, see the left picture in Figure 1. Let $k_0 = \omega\sqrt{\mu_0\varepsilon_0}$ be the wave number in Ω_{ext}. We define $\beta = k_0\cos\theta$, $\kappa_0^2 = k_0^2 - \beta^2$, and $\kappa_1^2 = \mu_1\varepsilon_1\omega^2 - \beta^2$, assuming that $\mu_1\varepsilon_1 > \mu_0\varepsilon_0\cos^2\theta$ such that $\kappa_1^2 > 0$. We denote by Ω_1 the horizontal cross section of the cylinder. Then, Ω_1 is a doubly-connected bounded domain in $\mathbb{R}^2$ with a C^2 smooth boundary Γ, consisting of two disjoint closed curves Γ_1 and Γ_0 such that $\Gamma = \Gamma_1 \cup \Gamma_0$, and $\Gamma_1 \cap \Gamma_0 = \emptyset$, see the right picture in Figure 1.

Let $\mathbf{x} = (x,y) \in \mathbb{R}^2$. Then, the exterior fields (the $z-$components of $\mathbf{E}^{ext}, \mathbf{H}^{ext}$) defined by $e^{ext}(\mathbf{x})$, $h^{ext}(\mathbf{x})$, for $\mathbf{x} \in \Omega_0$ and the interior fields $e^1(\mathbf{x})$, $h^1(\mathbf{x})$, $\mathbf{x} \in \Omega_1$ (the $z-$components of $\mathbf{E}^{int}, \mathbf{H}^{int}$), satisfy the system of Helmholtz equations

$$\begin{aligned} \Delta e^{ext} + \kappa_0^2 e^{ext} = 0, \quad \Delta h^{ext} + \kappa_0^2 h^{ext} = 0, \quad \text{in } \Omega_0, \\ \Delta e^1 + \kappa_1^2 e^1 = 0, \qquad \Delta h^1 + \kappa_1^2 h^1 = 0, \quad \text{in } \Omega_1. \end{aligned} \tag{2.4}$$

The boundary conditions (2.2) and (2.3) can also be rewritten only for the $z-$components of the

fields. Let $\mathbf{n} = (n_1, n_2)$ and $\boldsymbol{\tau} = (-n_2, n_1)$ be the normal and tangent vector on Γ, respectively. The vector $\mathbf{n}$ on Γ_j points into Ω_j, $j = 0, 1$. We define $\frac{\partial}{\partial n} = \mathbf{n} \cdot \nabla$, $\frac{\partial}{\partial \tau} = \boldsymbol{\tau} \cdot \nabla$, where ∇ is the two-dimensional gradient and we set

$$\tilde{\mu}_j = \frac{\mu_j}{\kappa_j^2}, \quad \tilde{\varepsilon}_j = \frac{\varepsilon_j}{\kappa_j^2}, \quad \beta_j = \frac{\beta}{\kappa_j^2}, \quad \text{for } j = 0, 1.$$

Then, the transmission conditions (2.2) take the form (see Gintides & Mindrinos (2016))

$$\begin{aligned} e^1 &= e^{ext}, && \text{on } \Gamma_0, \\ \tilde{\mu}_1 \omega \frac{\partial h^1}{\partial n} + \beta_1 \frac{\partial e^1}{\partial \tau} &= \tilde{\mu}_0 \omega \frac{\partial h^{ext}}{\partial n} + \beta_0 \frac{\partial e^{ext}}{\partial \tau}, && \text{on } \Gamma_0, \\ h^1 &= h^{ext}, && \text{on } \Gamma_0, \\ \tilde{\varepsilon}_1 \omega \frac{\partial e^1}{\partial n} - \beta_1 \frac{\partial h^1}{\partial \tau} &= \tilde{\varepsilon}_0 \omega \frac{\partial e^{ext}}{\partial n} - \beta_0 \frac{\partial h^{ext}}{\partial \tau}, && \text{on } \Gamma_0, \end{aligned} \tag{2.5}$$

and the impedance boundary condition results to (see Nakamura & Wang (2013))

$$\tilde{\mu}_1 \omega \frac{\partial h^1}{\partial n} + \beta_1 \frac{\partial e^1}{\partial \tau} + \lambda i h^1 = 0, \quad \text{on } \Gamma_1, \tag{2.6a}$$

$$\lambda \tilde{\varepsilon}_1 \omega \frac{\partial e^1}{\partial n} - \lambda \beta_1 \frac{\partial h^1}{\partial \tau} + i e^1 = 0, \quad \text{on } \Gamma_1. \tag{2.6b}$$

The exterior fields are decomposed as $e^{ext} = e^0 + e^{inc}$ and $h^{ext} = h^0 + h^{inc}$, where e^0 and h^0 is the scattered electric and magnetic field, respectively. The incident wave $(\mathbf{E}^{inc}, \mathbf{H}^{inc})$ reduces similarly to the fields ($z-$components), (see, e.g., Gintides & Mindrinos, 2016; Nakamura & Wang, 2012)

$$e^{inc}(\mathbf{x}) = \frac{1}{\sqrt{\varepsilon_0}} \sin\theta \, \mathrm{e}^{i\kappa_0(x\cos\phi + y\sin\phi)}, \quad h^{inc}(\mathbf{x}) = 0. \tag{2.7}$$

The scattered fields satisfy also the radiation conditions

$$\lim_{r\to\infty} \sqrt{r} \left(\frac{\partial e^0}{\partial r} - i\kappa_0 e^0 \right) = 0, \quad \lim_{r\to\infty} \sqrt{r} \left(\frac{\partial h^0}{\partial r} - i\kappa_0 h^0 \right) = 0, \tag{2.8}$$

where $r = |\mathbf{x}|$, uniformly over all directions.

The solutions e^0 and h^0 of (2.4) – (2.8) admit the asymptotic behavior

$$e^0(\mathbf{x}) = \frac{\mathrm{e}^{i\kappa_0 r}}{\sqrt{r}} e^\infty(\hat{\mathbf{x}}) + \mathcal{O}(r^{-3/2}), \quad h^0(\mathbf{x}) = \frac{\mathrm{e}^{i\kappa_0 r}}{\sqrt{r}} h^\infty(\hat{\mathbf{x}}) + \mathcal{O}(r^{-3/2}), \tag{2.9}$$

where $\hat{\mathbf{x}} = \mathbf{x}/r$. The pair (e^∞, h^∞) is called the far-field pattern of the scattered fields related to the scattering problem (2.4) – (2.8). We can formulate now the direct problem which we consider in this work.

Direct Problem: Given the coefficients λ, ε_0, μ_0, ε_1 and μ_1, the boundary curve $\Gamma = \Gamma_0 \cup \Gamma_1$, and the incident field (2.7), find the interior fields e^1 and h^1 and the scattered fields e^0 and h^0 which satisfy the system of Helmholtz equations (2.4), the boundary conditions (2.5) and (2.6) and the radiation conditions (2.8).

REMARK 2.1 Similar analysis holds also for the case of transverse electric polarized incident wave. The case of normal incidence $\theta = \pi/2$, resulting to $\beta_1 = \beta_0 = 0$, simplifies even more the scattering problem since it can be written as two decoupled problems for the electric and the magnetic field.

3. Uniqueness results

In this section we study the well-posedness of the direct problem. We use the integral equation method and we apply the Riesz-Fredholm theory. For the representation of the electric and magnetic (interior and exterior) fields we consider a hybrid method, meaning we combine the direct (Green's formulas) and the indirect (single layer ansatz) methods by Kleinman & Martin (1988). We define the "hole" as $\Omega_h := \mathbb{R}^2 \setminus (\overline{\Omega}_1 \cup \overline{\Omega}_0)$.

THEOREM 3.1 If κ_1^2 is not a Dirichlet eigenvalue in Ω_1 and the impedance parameter λ is positive, then the direct scattering problem (2.4) – (2.8) admits at most one solution.

Proof. It is enough to show that the corresponding homogeneous problem has only the trivial solution, meaning, $e^1 = h^1 = 0$, in Ω_1 and $e^0 = h^0 = 0$, in Ω_0. We consider a disk S_r with center at the origin, radius $r > 0$, and boundary Γ_r, which contains Ω_1. We set $\Omega_r = S_r \setminus (\overline{\Omega}_1 \cup \overline{\Omega}_h)$.

The transmission conditions on Γ_0 now read

$$e^1 = e^0, \qquad \text{on } \Gamma_0, \tag{3.1a}$$

$$\tilde{\mu}_1 \omega \frac{\partial h^1}{\partial n} + \beta_1 \frac{\partial e^1}{\partial \tau} = \tilde{\mu}_0 \omega \frac{\partial h^0}{\partial n} + \beta_0 \frac{\partial e^0}{\partial \tau}, \quad \text{on } \Gamma_0, \tag{3.1b}$$

$$h^1 = h^0, \qquad \text{on } \Gamma_0, \tag{3.1c}$$

$$\tilde{\varepsilon}_1 \omega \frac{\partial e^1}{\partial n} - \beta_1 \frac{\partial h^1}{\partial \tau} = \tilde{\varepsilon}_0 \omega \frac{\partial e^0}{\partial n} - \beta_0 \frac{\partial h^0}{\partial \tau}, \quad \text{on } \Gamma_0. \tag{3.1d}$$

We consider Green's first identity in Ω_1 for the electric fields e^1 and $\overline{e^1}$, together with the Helmholtz equation (2.4) and the boundary condition (2.6b), resulting in

$$\tilde{\varepsilon}_1 \int_{\Gamma_0} e^1 \frac{\partial \overline{e^1}}{\partial n}\, ds = \tilde{\varepsilon}_1 \int_{\Omega_1} \left(|\nabla e^1|^2 - \kappa_1^2 |e^1|^2 \right) d\mathbf{x} + \int_{\Gamma_1} e^1 \left(\frac{\beta_1}{\omega} \frac{\partial \overline{h^1}}{\partial \tau} + \frac{i}{\lambda \omega} \overline{e^1} \right) ds. \tag{3.2}$$

Similarly, Green's first identity in Ω_1 for the magnetic fields h^1 and $\overline{h^1}$, considering the Helmholtz equation (2.4) and the boundary condition (2.6a), gives

$$\tilde{\mu}_1 \int_{\Gamma_0} h^1 \frac{\partial \overline{h^1}}{\partial n}\, ds = \tilde{\mu}_1 \int_{\Omega_1} \left(|\nabla h^1|^2 - \kappa_1^2 |h^1|^2 \right) d\mathbf{x} + \int_{\Gamma_1} h^1 \left(-\frac{\beta_1}{\omega} \frac{\partial \overline{e^1}}{\partial \tau} + \frac{i\lambda}{\omega} \overline{h^1} \right) ds. \tag{3.3}$$

Applying Green's first identity in Ω_r for the exterior fields and considering the transmission conditions (3.1d) and (3.1b), we obtain

$$\tilde{\varepsilon}_0 \int_{\Gamma_r} e^0 \frac{\partial \overline{e^0}}{\partial n}\, ds = \tilde{\varepsilon}_0 \int_{\Omega_r} \left(|\nabla e^0|^2 - \kappa_0^2 |e^0|^2 \right) d\mathbf{x} + \int_{\Gamma_0} e^0 \left(\tilde{\varepsilon}_1 \frac{\partial \overline{e^1}}{\partial n} - \frac{\beta_1}{\omega} \frac{\partial \overline{h^1}}{\partial \tau} + \frac{\beta_0}{\omega} \frac{\partial \overline{h^0}}{\partial \tau} \right) ds, \tag{3.4}$$

and

$$\tilde{\mu}_0 \int_{\Gamma_r} h^0 \frac{\partial \overline{h^0}}{\partial n}\, ds = \tilde{\mu}_0 \int_{\Omega_r} \left(|\nabla h^0|^2 - \kappa_0^2 |h^0|^2 \right) d\mathbf{x} + \int_{\Gamma_0} h^0 \left(\tilde{\mu}_1 \frac{\partial \overline{h^1}}{\partial n} + \frac{\beta_1}{\omega} \frac{\partial \overline{e^1}}{\partial \tau} - \frac{\beta_0}{\omega} \frac{\partial \overline{e^0}}{\partial \tau} \right) ds. \tag{3.5}$$

We take the imaginary part of (3.4), and using (3.1a) and (3.2), we have that

$$\Im \left(\tilde{\varepsilon}_0 \int_{\Gamma_r} e^0 \frac{\partial \overline{e^0}}{\partial n}\, ds \right) = \Im \left(\frac{\beta_1}{\omega} \int_{\Gamma_1} e^1 \frac{\partial \overline{h^1}}{\partial \tau} ds - \frac{\beta_1}{\omega} \int_{\Gamma_0} e^1 \frac{\partial \overline{h^1}}{\partial \tau} ds + \frac{\beta_0}{\omega} \int_{\Gamma_0} e^0 \frac{\partial \overline{h^0}}{\partial \tau} ds \right) + \int_{\Gamma_1} \frac{1}{\lambda \omega} |e^1|^2 ds.$$

Analogously, the imaginary part of (3.5), considering (3.1c) and (3.3), takes the form

$$\Im\left(\tilde{\mu}_0\int_{\Gamma_r}h^0\frac{\partial\overline{h^0}}{\partial n}ds\right)=\Im\left(-\frac{\beta_1}{\omega}\int_{\Gamma_1}h^1\frac{\partial\overline{e^1}}{\partial\tau}ds+\frac{\beta_1}{\omega}\int_{\Gamma_0}h^1\frac{\partial\overline{e^1}}{\partial\tau}ds-\frac{\beta_0}{\omega}\int_{\Gamma_0}h^0\frac{\partial\overline{e^0}}{\partial\tau}ds\right)+\int_{\Gamma_1}\frac{\lambda}{\omega}|h^1|^2ds.$$

If $\lambda>0$, the addition of the above two equations, noting that

$$-\int_{\Gamma_j}e^k\frac{\partial\overline{h^k}}{\partial\tau}ds=\overline{\int_{\Gamma_j}h^k\frac{\partial\overline{e^k}}{\partial\tau}ds},\quad\text{for } k,j=0,1,$$

results to

$$\Im\left(\tilde{\varepsilon}_0\int_{\Gamma_r}e^0\frac{\partial\overline{e^0}}{\partial n}ds+\tilde{\mu}_0\int_{\Gamma_r}h^0\frac{\partial\overline{h^0}}{\partial n}ds\right)=\int_{\Gamma_1}\left(\frac{1}{\lambda\omega}|e^1|^2+\frac{\lambda}{\omega}|h^1|^2\right)ds\geqslant 0$$

The last equation, the radiation conditions (2.8) as $r\to\infty$ and Rellich's Lemma yield $e^0=h^0=0$ in Ω_0, (see Gintides & Mindrinos (2016); Wang & Nakamura (2012)). Hence, $e^0=h^0=0$ on Γ_0. Using the homogeneous transmission conditions (3.1a) and (3.1c) and the assumption on κ_1^2 we get also $e^1=h^1=0$ in Ω_1. This completes the proof. □

To prove existence of solutions we transform the direct problem to a system of boundary integral equations. We present the fundamental solution of the Helmholtz equation in $\mathbb{R}^2$, given by

$$\Phi_j(\mathbf{x},\mathbf{y})=\frac{i}{4}H_0^{(1)}(\kappa_j|\mathbf{x}-\mathbf{y}|),\quad \mathbf{x},\mathbf{y}\in\Omega_j,\quad \mathbf{x}\neq\mathbf{y},\tag{3.6}$$

where $H_0^{(1)}$ is the Hankel function of the first kind and zero order. We introduce the single- and double-layer potentials for a continuous density f, given by

$$\begin{aligned}(\mathscr{S}_{klj}f)(\mathbf{x})&=\int_{\Gamma_j}\Phi_k(\mathbf{x},\mathbf{y})f(\mathbf{y})ds(\mathbf{y}),\qquad \mathbf{x}\in\Omega_l,\\ (\mathscr{D}_{klj}f)(\mathbf{x})&=\int_{\Gamma_j}\frac{\partial\Phi_k}{\partial n(\mathbf{y})}(\mathbf{x},\mathbf{y})f(\mathbf{y})ds(\mathbf{y}),\quad \mathbf{x}\in\Omega_l,\end{aligned}$$

for $k,l,j=0,1$. The single-layer potential $\mathscr{S}$ is continuous in $\mathbb{R}^2$ and the their normal and tangential derivatives as $\mathbf{x}\to\Gamma_j$ satisfy the standard jump relations, see for instance Gintides & Mindrinos (2016). We define the integral operators

$$\begin{aligned}(S_{klj}f)(\mathbf{x})&=\int_{\Gamma_j}\Phi_k(\mathbf{x},\mathbf{y})f(\mathbf{y})ds(\mathbf{y}),&&\mathbf{x}\in\Gamma_l,\\ (D_{klj}f)(\mathbf{x})&=\int_{\Gamma_j}\frac{\partial\Phi_k}{\partial n(\mathbf{y})}(\mathbf{x},\mathbf{y})f(\mathbf{y})ds(\mathbf{y}),&&\mathbf{x}\in\Gamma_l,\\ (NS_{klj}f)(\mathbf{x})&=\int_{\Gamma_j}\frac{\partial\Phi_k}{\partial n(\mathbf{x})}(\mathbf{x},\mathbf{y})f(\mathbf{y})ds(\mathbf{y}),&&\mathbf{x}\in\Gamma_l,\\ (ND_{klj}f)(\mathbf{x})&=\int_{\Gamma_j}\frac{\partial^2\Phi_k}{\partial n(\mathbf{x})\partial n(\mathbf{y})}(\mathbf{x},\mathbf{y})f(\mathbf{y})ds(\mathbf{y}),&&\mathbf{x}\in\Gamma_l,\\ (TS_{klj}f)(\mathbf{x})&=\int_{\Gamma_j}\frac{\partial\Phi_k}{\partial\tau(\mathbf{x})}(\mathbf{x},\mathbf{y})f(\mathbf{y})ds(\mathbf{y}),&&\mathbf{x}\in\Gamma_l,\\ (TD_{klj}f)(\mathbf{x})&=\int_{\Gamma_j}\frac{\partial^2\Phi_k}{\partial\tau(\mathbf{x})\partial n(\mathbf{y})}(\mathbf{x},\mathbf{y})f(\mathbf{y})ds(\mathbf{y}),&&\mathbf{x}\in\Gamma_l.\end{aligned}\tag{3.7}$$

If we consider the direct method, meaning Green's second identity, for representing the interior and exterior electric and magnetic fields we get

$$\begin{aligned} u^1(\mathbf{x}) &= (\mathscr{S}_{110}\,\partial_n u^1)(\mathbf{x}) - (\mathscr{D}_{110}\,u^1)(\mathbf{x}) + (\mathscr{S}_{111}\,\partial_n u^1)(\mathbf{x}) + (\mathscr{D}_{111}\,u^1)(\mathbf{x}), && \mathbf{x}\in\Omega_1,\\ u^0(\mathbf{x}) &= (\mathscr{D}_{000}\,u^0)(\mathbf{x}) - (\mathscr{S}_{000}\,\partial_n u^0)(\mathbf{x}), && \mathbf{x}\in\Omega_0, \end{aligned}$$

for $u = e, h$. We observe that we have 8 unknown densities (4 for the electric and 4 for the magnetic field) for the interior fields and 4 unknown densities for the exterior fields and only 6 equations (the boundary conditions (2.5) and (2.6)). In order to reduce the number of the unknowns, motivated by Kleinman & Martin (1988), we consider a hybrid method, meaning a combination of the indirect and direct methods. We keep the direct method for the exterior fields and we consider a single-layer ansatz (indirect method) for the interior fields.

THEOREM 3.2 Let the assumptions of Theorem 3.1 still hold. If κ_1^2 is not a Dirichlet eigenvalue in Ω_h, and κ_0^2 is not a Dirichlet eigenvalue in $\mathbb{R}^2\setminus\overline{\Omega}_0$, then the problem (2.4) – (2.8) has a unique solution.

Proof. We search the solutions in the forms:

$$\begin{aligned} e^1(\mathbf{x}) &= (\mathscr{S}_{110}\,\psi_1^e)(\mathbf{x}) + (\mathscr{S}_{111}\,\psi_2^e)(\mathbf{x}), && \mathbf{x}\in\Omega_1,\\ h^1(\mathbf{x}) &= (\mathscr{S}_{110}\,\psi_1^h)(\mathbf{x}) + (\mathscr{S}_{111}\,\psi_2^h)(\mathbf{x}), && \mathbf{x}\in\Omega_1,\\ e^0(\mathbf{x}) &= (\mathscr{D}_{000}\,\phi_0^e)(\mathbf{x}) - (\mathscr{S}_{000}\,\psi_0^e)(\mathbf{x}), && \mathbf{x}\in\Omega_0,\\ h^0(\mathbf{x}) &= (\mathscr{D}_{000}\,\phi_0^h)(\mathbf{x}) - (\mathscr{S}_{000}\,\psi_0^h)(\mathbf{x}), && \mathbf{x}\in\Omega_0, \end{aligned} \tag{3.8}$$

with $\psi_0^u := \partial_n u^0|_{\Gamma_0}$ and $\phi_0^u := u^0|_{\Gamma_0}$, for $u = e, h$. We let $\mathbf{x}$ approach the boundaries Γ_j, and considering the jump relations of the potentials, (see, e.g., Colton & Kress, 2013b; Courant & Hilbert, 1962), we see that the boundary conditions (2.5) and (2.6) are satisfied if the densities ψ_k^u, ϕ_0^u, $k = 0,1,2$, $u = e, h$ solve the system of integral equations

$$\begin{aligned} S_{100}\psi_1^e + S_{101}\psi_2^e - \left(D_{000}+\tfrac{1}{2}\right)\phi_0^e + S_{000}\psi_0^e &= e^{inc},\\ \tilde{\mu}_1\omega\left(NS_{100}+\tfrac{1}{2}\right)\psi_1^h + \tilde{\mu}_1\omega NS_{101}\psi_2^h + \beta_1 TS_{100}\psi_1^e + \beta_1 TS_{101}\psi_2^e - \tilde{\mu}_0\omega ND_{000}\phi_0^h &\\ +\tilde{\mu}_0\omega\left(NS_{000}-\tfrac{1}{2}\right)\psi_0^h - \beta_0(TD_{000}+\tfrac{\partial_\tau}{2})\phi_0^e + \beta_0 TS_{000}\psi_0^e &= \beta_0\partial_\tau e^{inc},\\ S_{100}\psi_1^h + S_{101}\psi_2^h - \left(D_{000}+\tfrac{1}{2}\right)\phi_0^h + S_{000}\psi_0^h &= 0\\ \tilde{\varepsilon}_1\omega\left(NS_{100}+\tfrac{1}{2}\right)\psi_1^e + \tilde{\varepsilon}_1\omega NS_{101}\psi_2^e - \beta_1 TS_{100}\psi_1^h - \beta_1 TS_{101}\psi_2^h - \tilde{\varepsilon}_0\omega ND_{000}\phi_0^e &\\ +\tilde{\varepsilon}_0\omega\left(NS_{000}-\tfrac{1}{2}\right)\psi_0^e + \beta_0(TD_{000}+\tfrac{\partial_\tau}{2})\phi_0^h - \beta_0 TS_{000}\psi_0^h &= \tilde{\varepsilon}_0\omega\partial_n e^{inc},\\ \tilde{\mu}_1\omega NS_{110}\psi_1^h + \tilde{\mu}_1\omega\left(NS_{111}-\tfrac{1}{2}\right)\psi_2^h + \beta_1 TS_{110}\psi_1^e + \beta_1 TS_{111}\psi_2^e &\\ +i\lambda S_{110}\psi_1^h + i\lambda S_{111}\psi_2^h &= 0,\\ \lambda\tilde{\varepsilon}_1\omega NS_{110}\psi_1^e + \lambda\tilde{\varepsilon}_1\omega\left(NS_{111}-\tfrac{1}{2}\right)\psi_2^e - \lambda\beta_1 TS_{110}\psi_1^h - \lambda\beta_1 TS_{111}\psi_2^h &\\ +iS_{110}\psi_1^e + iS_{111}\psi_2^e &= 0. \end{aligned} \tag{3.9}$$

To simplify the above system, we set

$$\tilde{\varepsilon}_1\psi_1^e = -\tilde{\varepsilon}_0\psi_0^e, \quad \text{and} \quad \tilde{\mu}_1\psi_1^h = -\tilde{\mu}_0\psi_0^h, \tag{3.10}$$

and the system (3.9) admits the matrix form

$$(\mathbf{B}+\mathbf{C})\,\boldsymbol{\phi} = \mathbf{f}, \tag{3.11}$$

where $\boldsymbol{\phi} = (\phi_0^e, \psi_1^h, \phi_0^h, \psi_1^e, \psi_2^h, \psi_2^e)^\top \in \mathbb{C}^6$, $\quad \mathbf{f} = \left(e^{inc}, \beta_0 \partial_\tau e^{inc}, 0, \tilde{\varepsilon}_0 \omega \partial_n e^{inc}, 0, 0\right)^\top \in \mathbb{C}^6$, and

$$\mathbf{B} = \begin{pmatrix} -\frac{1}{2} & 0 & 0 & 0 & 0 & 0 \\ -\frac{\beta_0}{2}\partial_\tau & \tilde{\mu}_1\omega & 0 & 0 & 0 & 0 \\ 0 & 0 & -\frac{1}{2} & 0 & 0 & 0 \\ 0 & 0 & \frac{\beta_0}{2}\partial_\tau & \tilde{\varepsilon}_1\omega & 0 & 0 \\ 0 & 0 & 0 & 0 & -\frac{\tilde{\mu}_1\omega}{2} & 0 \\ 0 & 0 & 0 & 0 & 0 & -\frac{\lambda\tilde{\varepsilon}_1\omega}{2} \end{pmatrix}.$$

The operator $\mathbf{C} = (C_{kj})_{1\leqslant k,j\leqslant 6}$ has entries:

$$\begin{aligned}
&C_{11} = -D_{000}, && C_{14} = S_{100} - \frac{\tilde{\varepsilon}_1}{\tilde{\varepsilon}_0} S_{000}, && C_{16} = S_{101}, \\
&C_{21} = -\beta_0 T D_{000}, && C_{22} = \tilde{\mu}_1\omega(NS_{100} - NS_{000}), && C_{23} = -\tilde{\mu}_0\omega N D_{000}, \\
&C_{24} = \beta_1 T S_{100} - \beta_0 \frac{\tilde{\varepsilon}_1}{\tilde{\varepsilon}_0} T S_{000}, && C_{25} = \tilde{\mu}_1\omega N S_{101}, && C_{26} = \beta_1 T S_{101}, \\
&C_{32} = S_{100} - \frac{\tilde{\mu}_1}{\tilde{\mu}_0} S_{000}, && C_{33} = C_{11}, && C_{35} = C_{16}, \\
&C_{41} = -\tilde{\varepsilon}_0\omega N D_{000}, && C_{42} = -\beta_1 T S_{100} + \beta_0 \frac{\tilde{\mu}_1}{\tilde{\mu}_0} T S_{000}, && C_{43} = -C_{21}, \\
&C_{44} = \tilde{\varepsilon}_1\omega(NS_{100} - NS_{000}), && C_{45} = -C_{26}, && C_{46} = \tilde{\varepsilon}_1\omega N S_{101}, \\
&C_{52} = \tilde{\mu}_1\omega N S_{110} + i\lambda S_{110}, && C_{54} = \beta_1 T S_{110}, && C_{55} = \tilde{\mu}_1\omega N S_{111} + i\lambda S_{111}, \\
&C_{56} = \beta_1 T S_{111}, && C_{62} = -\lambda C_{54}, && C_{64} = \lambda\tilde{\varepsilon}_1\omega N S_{110} + i S_{110}, \\
&C_{65} = -\lambda C_{56}, && C_{66} = \lambda\tilde{\varepsilon}_1\omega N S_{111} + i S_{111}, &&
\end{aligned}$$

and the rest are zero. The special form of $\mathbf{B}$ and the boundedness of the tangential operator $\partial_\tau : H^{1/2}(\Gamma_0) \to H^{-1/2}(\Gamma_0)$ allow us to construct its bounded inverse, given by

$$\mathbf{B}^{-1} = \begin{pmatrix} -2 & 0 & 0 & 0 & 0 & 0 \\ -\frac{\beta_0}{\tilde{\mu}_1\omega}\partial_\tau & \frac{1}{\tilde{\mu}_1\omega} & 0 & 0 & 0 & 0 \\ 0 & 0 & -2 & 0 & 0 & 0 \\ 0 & 0 & \frac{\beta_0}{\tilde{\varepsilon}_1\omega}\partial_\tau & \frac{1}{\tilde{\varepsilon}_1\omega} & 0 & 0 \\ 0 & 0 & 0 & 0 & -\frac{2}{\tilde{\mu}_1\omega} & 0 \\ 0 & 0 & 0 & 0 & 0 & -\frac{2}{\lambda\tilde{\varepsilon}_1\omega} \end{pmatrix}.$$

Then, we rewrite (3.11) as

$$(\mathbf{I}+\mathbf{K})\,\boldsymbol{\phi}=\mathbf{g}, \tag{3.12}$$

where $\mathbf{I}$ is the identity operator, $\mathbf{g}=\mathbf{B}^{-1}\mathbf{f}=\left(-2e^{inc},\,0,\,0,\,\frac{\tilde{\varepsilon}_0}{\tilde{\varepsilon}_1}\partial_n e^{inc},\,0,\,0\right)^{\top}$, and the matrix $\mathbf{K}=\mathbf{B}^{-1}\mathbf{C}$ has now entries:

$$K_{1j}=-2C_{1j},\quad K_{3j}=-2C_{3j},\quad K_{5j}=-\frac{2}{\tilde{\mu}_1\omega}C_{5j},\quad K_{6j}=-\frac{2}{\lambda\tilde{\varepsilon}_1\omega}C_{6j},\quad \text{for } j=1,...,6,$$

and

$$\begin{aligned}
&K_{21}=0, && K_{22}=NS_{100}-NS_{000}, && K_{23}=-\frac{\tilde{\mu}_0}{\tilde{\mu}_1}ND_{000}, && K_{24}=\frac{\beta_1-\beta_0}{\tilde{\mu}_1\omega}TS_{100},\\
&K_{25}=NS_{101}, && K_{26}=\frac{\beta_1-\beta_0}{\tilde{\mu}_1\omega}TS_{101}, && K_{41}=-\frac{\tilde{\varepsilon}_0}{\tilde{\varepsilon}_1}ND_{000}, && K_{42}=\frac{\beta_0-\beta_1}{\tilde{\varepsilon}_1\omega}TS_{100},\\
&K_{43}=0, && K_{44}=K_{22}, && K_{45}=\frac{\beta_0-\beta_1}{\tilde{\varepsilon}_1\omega}TS_{101}, && K_{46}=K_{25}.
\end{aligned}$$

We define the product spaces:

$$\begin{aligned}
H_1&:=\left(H^{1/2}(\Gamma_0)\times H^{-1/2}(\Gamma_0)\right)^2\times\left(H^{-1/2}(\Gamma_1)\right)^2,\\
H_2&:=\left(H^{-1/2}(\Gamma_0)\times H^{-3/2}(\Gamma_0)\right)^2\times\left(H^{-3/2}(\Gamma_1)\right)^2,
\end{aligned}$$

and using the mapping properties of the integral operators (see, e.g., Colton & Kress, 2013b; Kress, 2014b), we see that the operator $\mathbf{K}:H_1\to H_2$ is compact. The last step is to prove uniqueness of solutions. Then, solvability of the system (3.12) follows from the Fredholm alternative theorem. It is sufficient to show that the operator $\mathbf{I}+\mathbf{K}$ is injective.

Let $\boldsymbol{\phi}$ solve $(\mathbf{I}+\mathbf{K})\,\boldsymbol{\phi}=\mathbf{0}$. Then, the fields (3.8) solve the problem (2.4) – (2.8) with $e^{inc}=\partial_n e^{inc}=\partial_\tau e^{inc}=0$, on Γ_0. Hence, by Theorem 3.1 we have $e^1=h^1=0$, in Ω_1 and $e^0=h^0=0$, in Ω_0. Continuity of the single-layer potential implies that e^1 and h^1 solve also

$$\Delta e^1+\kappa_1^2 e^1=0,\quad \Delta h^1+\kappa_1^2 h^1=0,\quad \text{in } \Omega_h,$$

and vanish on Γ_1. Thus, $e^1=h^1=0$, in Ω_h, if κ_1^2 is not a Dirichlet eigenvalue in Ω_h. The jump relation of the normal derivative of the single layer across the boundary Γ_1, gives $\psi_2^e=\psi_2^h=0$, on Γ_1.

We define

$$\tilde{e}(\mathbf{x})=(\mathscr{S}_{100}\,\psi_1^e)(\mathbf{x}),\quad \tilde{h}(\mathbf{x})=(\mathscr{S}_{100}\,\psi_1^h)(\mathbf{x}),\quad \mathbf{x}\in\Omega_0.$$

Again using the continuity of the single-layer potential we get $\tilde{e}=S_{100}\psi_1^e=e^1=0$, and $\tilde{h}=S_{100}\psi_1^h=h^1=0$, on Γ_0. Since $\tilde{e}$ and $\tilde{h}$ are also radiating solutions of the Helmholtz equation in Ω_0, we get $\tilde{e}=\tilde{h}=0$, in Ω_0 (see Colton & Kress (2013b)). Again the jump relation of the normal derivative of the single layer potential across the boundary Γ_0, results to $\psi_1^e=\psi_1^h=0$, on Γ_0. From (3.10) we have also $\psi_0^e=\psi_0^h=0$, on Γ_0.

Given now the representations (3.8), the homogeneous transmission conditions (3.1a) and (3.1c) and the jump relations of the double-layer potential we obtain the equations

$$\left(D_{000}-\frac{1}{2}\right)\phi_0^e=0,\quad \left(D_{000}-\frac{1}{2}\right)\phi_0^h=0,\quad \text{on } \Gamma_0.$$

This integral operator is injective if κ_0^2 is not a Dirichlet eigenvalue in $\mathbb{R}^2\setminus\overline{\Omega}_0$. Thus, $\phi_0^e=\phi_0^h=0$, on Γ_0, and therefore $\boldsymbol{\phi}=0$, which completes the proof. □

4. Numerical examples

We derive the numerical solution of (3.12) by a collocation method using trigonometric polynomial approximations (see Kress (2014b)). We use quadrature rules to handle the singularities (weak and strong) of the integral operators and the trapezoidal rule for approximating the smooth kernels (see Kress (2014a)). For the convergence and error analysis, see the work of Kress (1995). We do not present here the parametrized forms of the integral operators (3.7) since they can be found in many works, we refer the reader to the books of Colton & Kress (2013b); Kress (2014b) and to paper of Gintides & Mindrinos (2016, Section 4) for a complete list of all forms and special decompositions.

We present two different kind of problems. In the first case, we formulate a problem, as in the works of Gintides & Mindrinos (2016); Wang & Nakamura (2012), whose solutions (the scattered electric and magnetic fields) can be analytically calculated. In this way, we can see that the expected exponential convergence for analytical data is achieved (see Kress (1990, 2014b)). Secondly, we present results for the scattering problem of obliquely incident waves.

We assume that the smooth boundaries admit the following parametrization

$$\Gamma_j = \{\mathbf{x}^j(t) = (x_1^j(t), x_2^j(t)) : t \in [0, 2\pi]\}, \quad j = 0, 1,$$

where $\mathbf{x}^j : \mathbb{R} \to \mathbb{R}^2$ are C^2-smooth, 2π-periodic and injective in $[0, 2\pi)$. For the numerical implementation we consider equidistant grid points

$$t_k = \frac{k\pi}{n}, \quad k = 0, ..., 2n-1.$$

4.1 *Examples with analytic solution*

We construct a problem whose solutions are expressed analytically. Let $\mathbf{z}_1, \mathbf{z}_2 \in \Omega_1$ and $\mathbf{z}_3, \mathbf{z}_4 \in \Omega_0$ be four arbitrary points. We define the boundary functions

$$\begin{aligned}
f_1(\mathbf{x}) &= H_0^{(1)}(\kappa_1|\mathbf{r}_3(\mathbf{x})|) - H_0^{(1)}(\kappa_0|\mathbf{r}_1(\mathbf{x})|), && \mathbf{x} \in \Gamma_0,\\
f_2(\mathbf{x}) &= -\tilde{\mu}_1 \omega \kappa_1 H_1^{(1)}(\kappa_1|\mathbf{r}_4(\mathbf{x})|)\frac{\mathbf{n}(\mathbf{x})\cdot\mathbf{r}_4(\mathbf{x})}{|\mathbf{r}_4(\mathbf{x})|} - \beta_1 \kappa_1 H_1^{(1)}(\kappa_1|\mathbf{r}_3(\mathbf{x})|)\frac{\boldsymbol{\tau}(\mathbf{x})\cdot\mathbf{r}_3(\mathbf{x})}{|\mathbf{r}_3(\mathbf{x})|}\\
&\quad + \tilde{\mu}_0 \omega \kappa_0 H_1^{(1)}(\kappa_0|\mathbf{r}_2(\mathbf{x})|)\frac{\mathbf{n}(\mathbf{x})\cdot\mathbf{r}_2(\mathbf{x})}{|\mathbf{r}_2(\mathbf{x})|} + \beta_0 \kappa_0 H_1^{(1)}(\kappa_0|\mathbf{r}_1(\mathbf{x})|)\frac{\boldsymbol{\tau}(\mathbf{x})\cdot\mathbf{r}_1(\mathbf{x})}{|\mathbf{r}_1(\mathbf{x})|}, && \mathbf{x} \in \Gamma_0,\\
f_3(\mathbf{x}) &= H_0^{(1)}(\kappa_1|\mathbf{r}_4(\mathbf{x})|) - H_0^{(1)}(\kappa_0|\mathbf{r}_2(\mathbf{x})|),, && \mathbf{x} \in \Gamma_0,\\
f_4(\mathbf{x}) &= -\tilde{\varepsilon}_1 \omega \kappa_1 H_1^{(1)}(\kappa_1|\mathbf{r}_3(\mathbf{x})|)\frac{\mathbf{n}(\mathbf{x})\cdot\mathbf{r}_3(\mathbf{x})}{|\mathbf{r}_3(\mathbf{x})|} + \beta_1 \kappa_1 H_1^{(1)}(\kappa_1|\mathbf{r}_4(\mathbf{x})|)\frac{\boldsymbol{\tau}(\mathbf{x})\cdot\mathbf{r}_4(\mathbf{x})}{|\mathbf{r}_4(\mathbf{x})|}\\
&\quad + \tilde{\varepsilon}_0 \omega \kappa_0 H_1^{(1)}(\kappa_0|\mathbf{r}_1(\mathbf{x})|)\frac{\mathbf{n}(\mathbf{x})\cdot\mathbf{r}_1(\mathbf{x})}{|\mathbf{r}_1(\mathbf{x})|} - \beta_0 \kappa_0 H_1^{(1)}(\kappa_0|\mathbf{r}_2(\mathbf{x})|)\frac{\boldsymbol{\tau}(\mathbf{x})\cdot\mathbf{r}_2(\mathbf{x})}{|\mathbf{r}_2(\mathbf{x})|}, && \mathbf{x} \in \Gamma_0,\\
f_5(\mathbf{x}) &= -\tilde{\mu}_1 \omega \kappa_1 H_1^{(1)}(\kappa_1|\mathbf{r}_4(\mathbf{x})|)\frac{\mathbf{n}(\mathbf{x})\cdot\mathbf{r}_4(\mathbf{x})}{|\mathbf{r}_4(\mathbf{x})|} - \beta_1 \kappa_1 H_1^{(1)}(\kappa_1|\mathbf{r}_3(\mathbf{x})|)\frac{\boldsymbol{\tau}(\mathbf{x})\cdot\mathbf{r}_3(\mathbf{x})}{|\mathbf{r}_3(\mathbf{x})|}\\
&\quad + i\lambda H_0^{(1)}(\kappa_1|\mathbf{r}_4(\mathbf{x})|), && \mathbf{x} \in \Gamma_1,\\
f_6(\mathbf{x}) &= -\lambda \tilde{\varepsilon}_1 \omega \kappa_1 H_1^{(1)}(\kappa_1|\mathbf{r}_3(\mathbf{x})|)\frac{\mathbf{n}(\mathbf{x})\cdot\mathbf{r}_3(\mathbf{x})}{|\mathbf{r}_3(\mathbf{x})|} + \lambda\beta_1 \kappa_1 H_1^{(1)}(\kappa_1|\mathbf{r}_4(\mathbf{x})|)\frac{\boldsymbol{\tau}(\mathbf{x})\cdot\mathbf{r}_4(\mathbf{x})}{|\mathbf{r}_4(\mathbf{x})|}\\
&\quad + iH_0^{(1)}(\kappa_1|\mathbf{r}_3(\mathbf{x})|), && \mathbf{x} \in \Gamma_1,
\end{aligned}$$

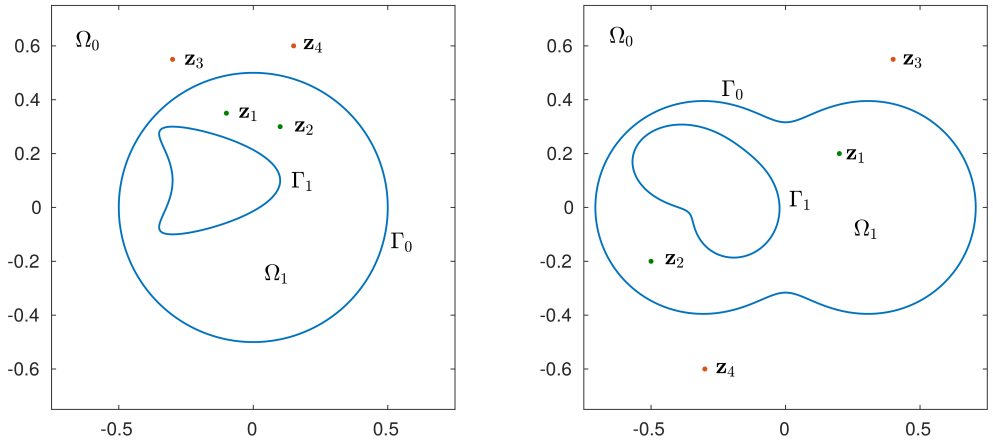

FIG. 2. The parametrization of the boundary $\Gamma = \Gamma_1 \cup \Gamma_0$ and the source points in the first (left) and in the second example (right).

where $\mathbf{r}_k(\mathbf{x}) = \mathbf{x} - \mathbf{z}_k, k = 1,2,3,4$. Then, the fields

$$\begin{aligned} e^0(\mathbf{x}) &= H_0^{(1)}(\kappa_0|\mathbf{x}-\mathbf{z}_1|), \quad h^0(\mathbf{x}) = H_0^{(1)}(\kappa_0|\mathbf{x}-\mathbf{z}_2|), \quad \mathbf{x} \in \Omega_0, \\ e^1(\mathbf{x}) &= H_0^{(1)}(\kappa_1|\mathbf{x}-\mathbf{z}_3|), \quad h^1(\mathbf{x}) = H_0^{(1)}(\kappa_1|\mathbf{x}-\mathbf{z}_4|), \quad \mathbf{x} \in \Omega_1, \end{aligned} \tag{4.1}$$

solve the equations

$$\begin{aligned} \Delta e^0 + \kappa_0^2 e^0 = 0, \quad \Delta h^0 + \kappa_0^2 h^0 = 0, \quad \text{in } \Omega_0, \\ \Delta e^1 + \kappa_1^2 e^1 = 0, \quad \Delta h^1 + \kappa_1^2 h^1 = 0, \quad \text{in } \Omega_1, \end{aligned}$$

with boundary conditions

$$\begin{aligned} e^1 - e^0 &= f_1, && \text{on } \Gamma_0, \\ \tilde{\mu}_1 \omega \frac{\partial h^1}{\partial n} + \beta_1 \frac{\partial e^1}{\partial \tau} - \tilde{\mu}_0 \omega \frac{\partial h^0}{\partial n} - \beta_0 \frac{\partial e^0}{\partial \tau} &= f_2, && \text{on } \Gamma_0, \\ h^1 - h^0 &= f_3, && \text{on } \Gamma_0, \\ \tilde{\varepsilon}_1 \omega \frac{\partial e^1}{\partial n} - \beta_1 \frac{\partial h^1}{\partial \tau} - \tilde{\varepsilon}_0 \omega \frac{\partial e^0}{\partial n} + \beta_0 \frac{\partial h^0}{\partial \tau} &= f_4, && \text{on } \Gamma_0, \\ \tilde{\mu}_1 \omega \frac{\partial h^1}{\partial n} + \beta_1 \frac{\partial e^1}{\partial \tau} + \lambda i h^1 &= f_5, && \text{on } \Gamma_1, \\ \lambda \tilde{\varepsilon}_1 \omega \frac{\partial e^1}{\partial n} - \lambda \beta_1 \frac{\partial h^1}{\partial \tau} + i e^1 &= f_6, && \text{on } \Gamma_1. \end{aligned}$$

and e^0, h^0 satisfy in addition the radiation conditions (2.8).

As in the proof of Theorem 3.2 we derive a system of the form (3.12), where now the right-hand side is given by

$$\mathbf{g}_f = \left(-2f_1, -\frac{\beta_0}{\tilde{\mu}_1\omega}\partial_\tau f_1 + \frac{1}{\tilde{\mu}_1\omega} f_2, -2f_3, \frac{\beta_0}{\tilde{\varepsilon}_1\omega}\partial_\tau f_3 + \frac{1}{\tilde{\varepsilon}_1\omega} f_4, -\frac{2}{\tilde{\mu}_1\omega} f_5, -\frac{2}{\lambda\tilde{\varepsilon}_1\omega} f_6 \right)^\top.$$

Initially we compare the exact near-fields, the scattered and the interior fields given by (4.1), with the computed near-fields e_n^1, h_n^1, e_n^0 and h_n^0, given by (3.8) where now the densities solve (3.12) with $\mathbf{g}$ replaced by $\mathbf{g}_f$. Then, using the asymptotic behavior of the Hankel functions (see Colton & Kress (2013b)), we can construct the exact and the computed far-field pattern of the scattered fields, which will be needed for the corresponding inverse problem. We see from (4.1) that the exact values of the far-field patterns of e^0 and h^0 are given by

$$e^\infty(\hat{\mathbf{x}}) = \frac{-4ie^{i\pi/4}}{\sqrt{8\pi\kappa_0}} \mathrm{e}^{-i\kappa_0\hat{\mathbf{x}}\cdot\mathbf{z}_1}, \quad h^\infty(\hat{\mathbf{x}}) = \frac{-4ie^{i\pi/4}}{\sqrt{8\pi\kappa_0}} e^{-i\kappa_0\hat{\mathbf{x}}\cdot\mathbf{z}_2}, \quad \hat{\mathbf{x}} \in S, \tag{4.2}$$

where S is the unit circle. The representations (3.8), where again the densities solve (3.12) with $\mathbf{g}_f$, result in

$$\begin{aligned} e_n^\infty(\hat{\mathbf{x}}(t)) &= \frac{\mathrm{e}^{i\pi/4}}{\sqrt{8\pi\kappa_0}} \int_0^{2\pi} \mathrm{e}^{-i\kappa_0\hat{\mathbf{x}}\cdot\mathbf{x}^0(t)} \left[-i\kappa_0(\hat{\mathbf{x}}\cdot\mathbf{n}(\mathbf{x}^0(t)))\phi_0^e(t) - \psi_0^e(t) \right] |\mathbf{x}^{0\prime}(t)| dt, \\ h_n^\infty(\hat{\mathbf{x}}(t)) &= \frac{\mathrm{e}^{i\pi/4}}{\sqrt{8\pi\kappa_0}} \int_0^{2\pi} \mathrm{e}^{-i\kappa_0\hat{\mathbf{x}}\cdot\mathbf{x}^0(t)} \left[-i\kappa_0(\hat{\mathbf{x}}\cdot\mathbf{n}(\mathbf{x}^0(t)))\phi_0^h(t) - \psi_0^h(t) \right] |\mathbf{x}^{0\prime}(t)| dt. \end{aligned} \tag{4.3}$$

In the first example, we set the outer boundary curve Γ_0 to be a circle with center $(0,0)$ and radius 0.5, and the inner Γ_1 is a kite-shaped boundary of the form

$$\Gamma_1 = \left\{ \mathbf{x}^1(t) = (0.2\cos t + 0.1\cos 2t - 0.2, 0.2\sin t + 0.1), t \in [0, 2\pi] \right\}.$$

We consider the interior points $\mathbf{z}_1 = (-0.1, 0.35), \mathbf{z}_2 = (0.1, 0.3) \in \Omega_1$, and the exterior points $\mathbf{z}_3 = (-0.3, 0.55)$, $\mathbf{z}_4 = (0.15, 0.6) \in \Omega_0$, see the left picture in Figure 2. We set $\omega = 1$, $\lambda = 2$ and $\theta = \pi/3$. The parameters are given by $(\varepsilon_0, \mu_0) = (1,1)$ and $(\varepsilon_1, \mu_1) = (3,2)$, resulting to the wave numbers $(\kappa_0, \kappa_1) = (0.86, 2.39)$.

The exact and computed interior fields at specific positions for increasing number of quadrature points n are shown in Table 1. The scattered fields at different positions are presented in Table 2. Table 3 shows the computed far-field of the electric and magnetic scattered fields at direction $t = 0$ for different values of n. The exponential convergence is clearly exhibited, as we see also in Figure 3 and Figure 4 where we plot the logarithm of the absolute error and the L^2 norm of the difference between the exact and the computed near- and far-fields, respectively.

In the second example, both boundaries admit the following parametrization

$$\Gamma_j = \left\{ \mathbf{x}^j(t) = r_j(t)(\cos t, \sin t) + \mathbf{a}^j, t \in [0, 2\pi] \right\}, \quad j = 0, 1.$$

We consider a peanut-shaped outer boundary with radial function

$$r_0(t) = \left(0.5\cos^2 t + 0.1\sin^2 t \right)^{1/2}, \quad \text{and} \quad \mathbf{a}^0 = (0,0),$$

n	$e_n^1(0.2, 0.3)$	$h_n^1(0, -0.2)$
8	$0.604945956508 + i0.284320213602$	$0.232651970281 + i0.491947424153$
16	$0.597795060635 + i0.308480211402$	$0.251943884858 + i0.504656386375$
32	$0.598782366842 + i0.308159788441$	$0.251777972181 + i0.504552637621$
64	$0.598781975739 + i0.308160170939$	$0.251778317958 + i0.504552845467$
	$e^1(0.2, 0.3)$	$h^1(0, -0.2)$
	$0.598781975712 + i0.308160170944$	$0.251778317952 + i0.504552845463$

Table 1. The computed and the exact interior electric and magnetic fields of the first example.

n	$e_n^0(1, 0)$	$h_n^0(-0.5, 0.6)$
8	$0.847357910341 - i0.071675589965$	$0.944884523579 - i0.572087978672$
16	$0.837799503290 - i0.066361103779$	$0.958761357922 - i0.591361698290$
32	$0.838237289559 - i0.065951591297$	$0.958713913359 - i0.591017903163$
64	$0.838237055126 - i0.065951532474$	$0.958714351829 - i0.591018302227$
	$e^0(1, 0)$	$h^0(-0.5, 0.6)$
	$0.838237055118 - i0.065951532477$	$0.958714351843 - i0.591018302238$

Table 2. The computed and the exact scattered electric and magnetic fields of the first example.

and an apple-shaped inner boundary curve with

$$r_1(t) = \frac{0.45 + 0.3\cos t - 0.1\sin 2t}{1 + 0.7\cos t}, \quad \text{and} \quad \mathbf{a}^1 = (-0.25, 0.05).$$

The source points are now: $\mathbf{z}_1 = (0.2, 0.2), \mathbf{z}_2 = (-0.5, -0.2) \in \Omega_1$, and $\mathbf{z}_3 = (0.4, 0.55), \mathbf{z}_4 = (-0.3, -0.6) \in \Omega_0$, see the right picture in Figure 2. We set $\omega = 2$ and $\theta = \pi/4$, and we choose the parameters to be $(\varepsilon_0, \mu_0) = (2, 1)$ and $(\varepsilon_1, \mu_1) = (4, 2)$. The wave numbers are now $(\kappa_0, \kappa_1) = (2, 5.29)$. Here, the impedance function is given by

$$\lambda(\mathbf{x}^1(t)) = \frac{1}{1 + 0.2\cos t}.$$

The computed and the exact interior electric and scattered magnetic fields for increasing number of quadrature points n, at specific positions, are presented in Table 4. The computed far-field of the electric and magnetic scattered fields for varying n, and the exact far-fields at direction $t = \pi/4$ are given in Table 5. Their L^2 norm difference is presented in Figure 5. Table 6 shows the L^2 norm of the difference between the exact and the computed far-fields with respect to n, for both examples. Again the exponential convergence is guaranteed independently of the different parameters.

The computed values are accurate also with respect to the wave number. We use the parametrization of the second example. In Table 7 we see the absolute error between the computed and the exact scattered electric and magnetic fields at the position $(0.6, -0.6)$, for $(\varepsilon_0, \mu_0) = (1, 1)$, $(\varepsilon_1, \mu_1) = (3, 1)$,

n	$e_n^\infty(\hat{\mathbf{x}}(0))$	$h_n^\infty(\hat{\mathbf{x}}(0))$
8	$0.550084263052 - i0.665877312380$	$0.646238687778 - i0.549065505420$
16	$0.550961953612 - i0.656336124631$	$0.656591070845 - i0.551308759662$
32	$0.551551006183 - i0.656427458763$	$0.656427073431 - i0.551550848571$
64	$0.551550951843 - i0.656427255249$	$0.656427255242 - i0.551550951840$
	$e^\infty(\hat{\mathbf{x}}(0))$	$h^\infty(\hat{\mathbf{x}}(0))$
	$0.551550951838 - i0.656427255240$	$0.656427255240 - i0.551550951838$

Table 3. The computed and the exact far-fields of the electric and magnetic scattered fields of the first example.

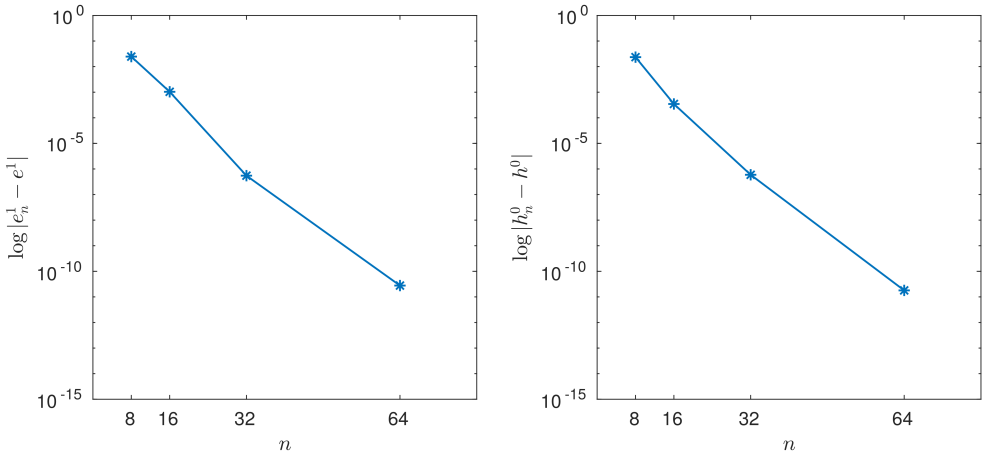

FIG. 3. The absolute error (in logarithmic scale) between the computed and the exact values of the interior electric (left) and the scattered magnetic (right) fields of the first example.

$\theta = \pi/3$, and different values of $k_0 = \omega$, as n increases. Table 8 presents the L^2 norm of the difference between the computed and the exact far-fields of the scattered electric and magnetic fields for varying n and different sets of wave numbers (κ_0, κ_1). Here, we keep fixed $\omega = 2$ and $\theta = \pi/3$.

4.2 *Examples with oblique incidence*

We consider obliquely incident waves of the form (2.7) and we vary the polar angle ϕ, which corresponds to the incident direction $(\cos\phi, \sin\phi)$ in two dimensions. We restrict the computation domain to the rectangular domain $[-c, c]^2$, where we consider a uniform-space grid of the form $\mathbf{x}_{kj} = (-c + k\delta, -c + j\delta)$, with $\delta = 2c/(2m-1)$, for $k, j = 0, ..., 2m-1$. We use $m = 128$.

In the third example we consider the same parametrization as in the first example and we set $\omega = 6$ and $\theta = \pi/4$, while keeping all the other parameters the same. The values of the norms of the interior

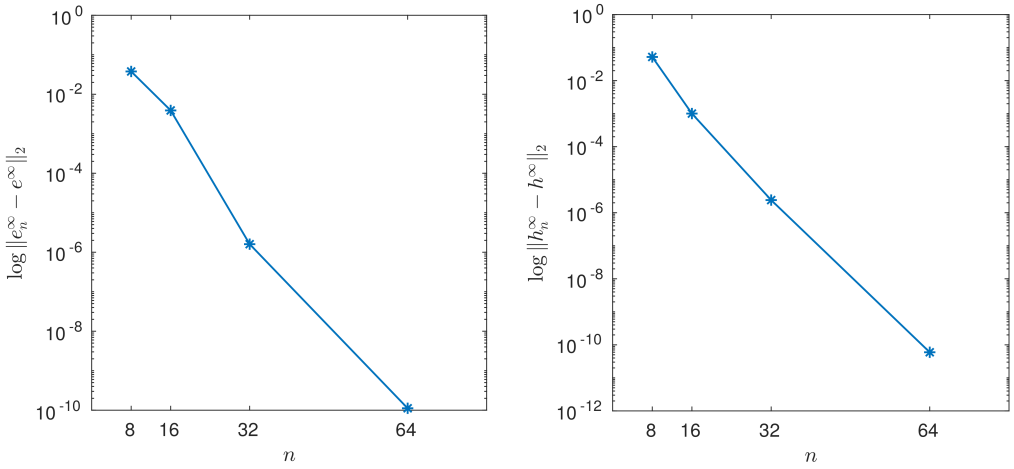

FIG. 4. The L^2 norm (in logarithmic scale) of the difference between the computed and the exact far-field of the electric (left) and the magnetic (right) scattered fields of the first example.

and exterior fields are given in Figure 6 for $c = 0.8$ and $\phi = \pi/2$.

In the last example we consider the setup of the second example, where now $\mathbf{a}^1 = (0.25, -0.05)$. We set $\omega = 1$, and $\theta = \phi = \pi/6$. The parameters are given by $(\varepsilon_0, \mu_0) = (1,1)$ and $(\varepsilon_1, \mu_1) = (6,4)$. In Figure 7 we see the results for $c = 1$.

All algorithms were implemented in Matlab 2017b using an Intel Core i7-4820K at 3.70GHz workstation equipped with 64 GB RAM. The matrix $\mathbf{I} + \mathbf{K}$ is dense of size $12n \times 12n$ and has a condition number of order 10^3 for $n = 16$, and of order 10^4 for $n = 64$, in all examples. However, the computations are considerably fast because of the exponential convergence. For example, the values for $n = 64$ presented in Tables 1 and 2 were obtained in approximately 0.7 sec.

5. Conclusions

We addressed the direct electromagnetic scattering problem for a infinitely long, penetrable and doubly-connected cylinder. The cylinder was placed in a homogeneous dielectric medium and was illuminated by a time-harmonic electromagnetic wave at oblique incidence. We considered transmission conditions on the outer boundary and impedance boundary condition on the inner boundary. We proved the well-posedness of the problem using Green's formulas and the integral representation of the solutions (hybrid method). We presented numerical results which showed the feasibility of the proposed method.

Acknowledgements

The author would like to thank Drossos Gintides for discussions and his suggestions on this topic.

REFERENCES

n	$e_n^1(0.3, 0.1)$	$h_n^0(0, 0.7)$
8	$0.052891297598 + i0.532859083462$	$0.147230201766 + i0.573325863089$
16	$-0.015687011145 + i0.506515315775$	$0.188858594306 + i0.517179634229$
32	$-0.017746551481 + i0.506112420391$	$0.189915882635 + i0.515726095529$
64	$-0.017747386434 + i0.506111025685$	$0.189917768280 + i0.515725452050$
	$e^1(0.3, 0.1)$	$h^0(0, 0.7)$
	$-0.017747386432 + i0.506111025684$	$0.189917768283 + i0.515725452050$

Table 4. The computed and the exact interior electric and scattered magnetic fields of the second example.

n	$e_n^\infty(\hat{\mathbf{x}}(\pi/4))$	$h_n^\infty(\hat{\mathbf{x}}(\pi/4))$
8	$0.110995105311 - i0.558817682095$	$0.533445748875 + i0.122603921042$
16	$0.123115240894 - i0.551055700217$	$0.552938285062 + i0.114751031182$
32	$0.122965211004 - i0.550626647288$	$0.552427942024 + i0.114603756425$
64	$0.122964711410 - i0.550626521274$	$0.552427483456 + i0.114602625221$
	$e^\infty(\hat{\mathbf{x}}(\pi/4))$	$h^\infty(\hat{\mathbf{x}}(\pi/4))$
	$0.122964711410 - i0.550626521275$	$0.552427483455 + i0.114602625221$

Table 5. The computed and the exact far-fields of the electric and magnetic scattered fields of the second example.

Boubendir, Y., Turc, C. & Domnguez, V. (2016) High-order Nystrm discretizations for the solution of integral equation formulations of two-dimensional Helmholtz transmission problems. *IMA Journal of Numerical Analysis*, **36**(1), 463–492.

Cakoni, F. & Colton, D. (2006) *Qualitative Methods in Inverse Scattering Theory*. Springer-Verlag, Berlin.

Cakoni, F. & Kress, R. (2012) Integral equation methods for the inverse obstacle problem with generalized impedance boundary condition. *Inverse Problems*, **29**(1), 015005.

Cangellaris, A. C. & Lee, R. (1991) Finite element analysis of electromagnetic scattering from inhomogeneous cylinders at oblique incidence. *IEEE Transactions on Antennas and Propagation*, **39**(5), 645–650.

Chapko, R., Gintides, D. & Mindrinos, L. (2017) The inverse scattering problem by an elastic inclusion. *Advances in Computation Mathematics*, pages 1–24.

Chapko, R., Ivanyshyn, O. & Protsyuk, O. (2013) On a nonlinear integral equation approach for the surface reconstruction in semi-infinite-layered domains. *Inverse Problems in Science and Engineering*, **21**(3), 547–561.

Colton, D. & Kress, R. (2013a) *Integral equation methods in scattering theory*. Classics in Applied Mathematics. Society for Industrial and Applied Mathematics, Philadelphia.

Colton, D. & Kress, R. (2013b) *Inverse Acoustic and Electromagnetic Scattering Theory*. Number 93 in Applied Mathematical Sciences. Springer, Berlin, 3 edition.

Courant, R. & Hilbert, D. (1962) *Methods of mathematical physics*. Wiley-Interscience, New York.

Erturk, V. & Rojas, R. G. (2000) Efficient computation of surface fields excited on a dielectric-coated circular cylinder. *IEEE Transactions on Antennas and Propagation*, **48**(10), 1507–1516.

Gintides, D. & Mindrinos, L. (2016) The direct scattering problem of obliquely incident electromagnetic waves by

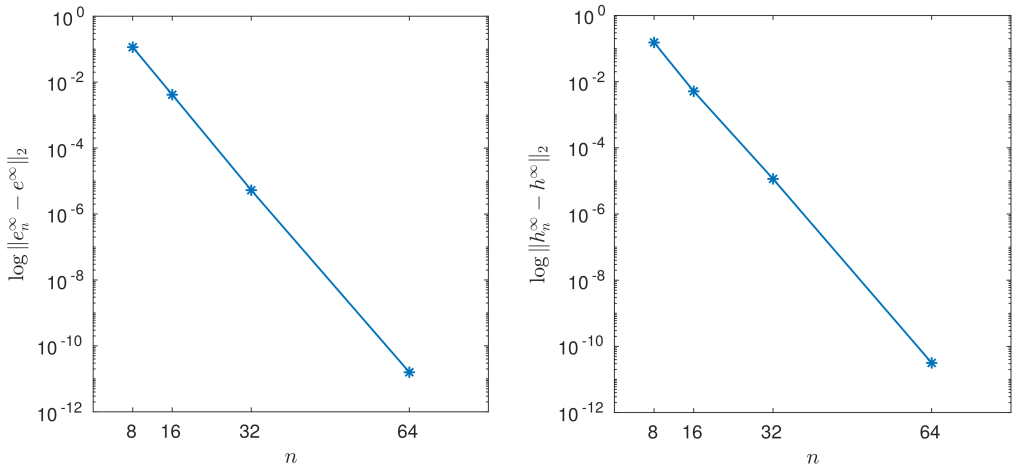

FIG. 5. The L^2 norm (in logarithmic scale) of the difference between the computed and the exact far-field of the electric (left) and the magnetic (right) scattered fields of the second example.

n	$\|e_n^\infty - e^\infty\|_2$	$\|h_n^\infty - h^\infty\|_2$	$\|e_n^\infty - e^\infty\|_2$	$\|h_n^\infty - h^\infty\|_2$
8	0.0377711463147	0.0520836564980	0.1147876797398	0.1529965493475
16	0.0038935330831	0.0010061270829	0.0041568722073	0.0051035937561
32	0.0000016001748	0.0000024170377	0.0000052833063	0.0000115204056
64	0.0000000001118	0.0000000000596	0.0000000000158	0.0000000000316

Table 6. The L^2 norm of the difference between the computed and the exact far-fields of the electric and magnetic scattered fields of the first (first two columns) and of the second (last two columns) example.

a penetrable homogeneous cylinder. *Journal of Integral Equations and Applications*, **28**(1), 91–122.

Gintides, D. & Mindrinos, L. (2017) The inverse electromagnetic scattering problem by a penetrable cylinder at oblique incidence. *Applicable Analysis*, pages 1–18.

Ivanyshyn, O. & Louër, F. L. (2016) Material derivatives of boundary integral operators in electromagnetism and application to inverse scattering problems. *Inverse Problems*, **32**(9), 095003.

Kirsch, A. & Hettlich, F. (2015) *Mathematical Theory of Time-harmonic Maxwell's Equations*. Number 190 in Applied Mathematical Sciences. Springer, Switzerland.

Kleinman, R. E. & Martin, P. A. (1988) On single integral equations for the transmission problem of acoustics. *SIAM Journal on Applied Mathematics*, **48**(2), 307–325.

Kress, R. (1990) Numerical Solution of Boundary Integral Equations in Time-Harmonic Electromagnetic Scattering. *Electromagnetics*, **10**(1–2), 1–20.

Kress, R. (1995) On the numerical solution of a hypersingular integral equation in scattering theory. *SIAM Journal on Applied Mathematics*, **61**(3), 345–360.

Kress, R. (2014a) A collocation method for a hypersingular boundary integral equation via trigonometric differentiation. *Journal of Integral Equations and Applications*, **26**(2), 197–213.

	$\lvert e_n^0 - e^0\rvert$		
n \ k_0	0.1	1	10
16	0.004228025039578	0.000559126168652	0.004006547188780
32	0.000002177667052	0.000000549213937	0.000002594744892
64	0.000000000004205	0.000000000000984	0.000000000006334
	$\lvert h_n^0 - h^0\rvert$		
16	0.015766587442913	0.000544231265856	0.007559468207215
32	0.000001455838646	0.000000928965969	0.000001553058964
64	0.000000000001864	0.000000000001713	0.000000000004229

Table 7. The absolute error between the computed and the exact, electric and magnetic, scattered fields of the second example, for different values of n and k_0, at the position $(0.6, -0.6)$.

	$\lVert e_n^\infty - e^\infty\rVert_2$			
n \ (κ_0, κ_1)	$(1.73, 1.84)$	$(1.73, 19.97)$	$(1.81, 1.70)$	$(3, 0.99)$
16	0.003720064110	0.087831672702	0.003892601878	0.011471300141
32	0.000005028601	0.000033279914	0.000005172048	0.000015731178
64	0.000000000013	0.000000000048	0.000000000016	0.000000000769
	$\lVert h_n^\infty - h^\infty\rVert_2$			
16	0.002461277234	0.071396442491	0.002387063488	0.014090335292
32	0.000004061484	0.000031104515	0.000003762957	0.000023579662
64	0.000000000012	0.000000000072	0.000000000012	0.000000000965

Table 8. The L^2 norm of the difference between the computed and the exact far-fields of the scattered electric and magnetic fields for different pairs (κ_0, κ_1) and increasing number of n.

Kress, R. (2014b) *Linear Integral Equations*. Springer, New York, 3rd edition.

Lucido, M., Panariello, G. & Schettino, F. (2010) Scattering by polygonal cross-section dielectric cylinders at oblique incidence. *IEEE Transactions on Antennas and Propagation*, **58**(2), 540–551.

Nakamura, G. & Wang, H. (2012) Inverse scattering for obliquely incident polarized electromagnetic waves. *Inverse problems*, **28**(10), 105004.

Nakamura, G. & Wang, H. (2013) The direct electromagnetic scattering problem from an imperfectly conducting cylinder at oblique incidence. *Journal of Mathematical Analysis and Applications*, **397**, 142–155.

Rojas, R. (1988) Scattering by an inhomogeneous dielectric/ferrite cylinder of arbitrary cross-section shape-oblique incidence case. *IEEE Transactions on Antennas and Propagation*, **36**(2), 238–246.

Sarabandi, K. & Senior, T. (1990) Low-frequency scattering from cylindrical structures at oblique incidence. *IEEE Transactions on Geoscience and Remote Sensing*, **28**(5), 879–885.

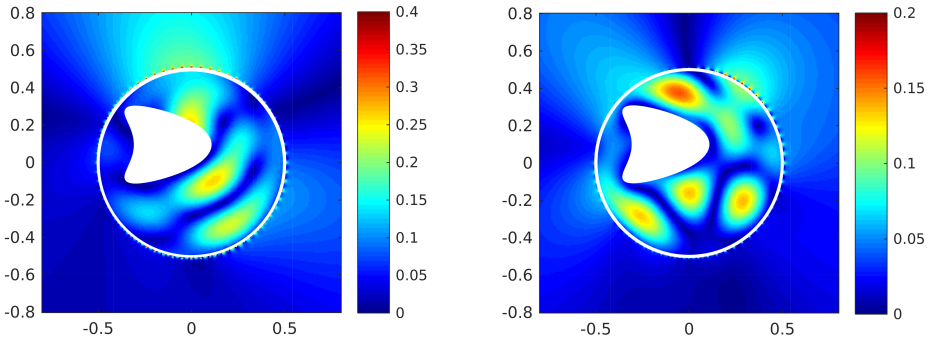

FIG. 6. The norms of the electric fields e^0 and e^1 (left) and those of the magnetic fields h^0 and h^1 (right) for $\phi = \pi/2$.

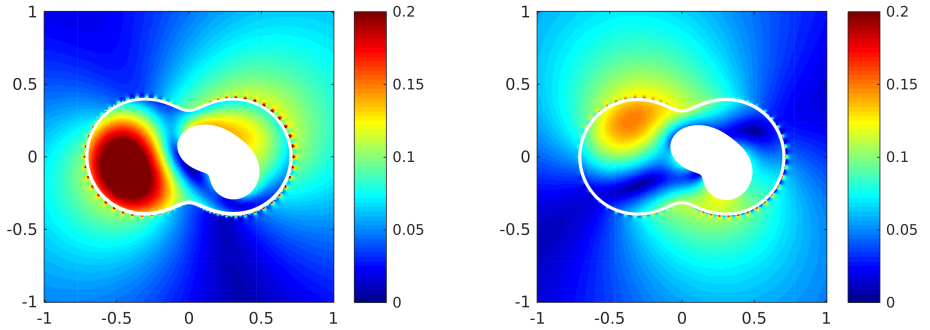

FIG. 7. The norms of the electric fields e^0 and e^1 (left) and those of the magnetic fields h^0 and h^1 (right) for $\phi = \pi/6$.

Tsalamengas, J. (2007) Exponentially converging Nyström methods applied to the integral-integrodifferential equations of oblique scattering/ hybrid wave propagation in presence of composite dielectric cylinders of arbitrary cross section. *IEEE Transactions on Antennas and Propagation*, **55**, 3239–3250.

Tsitsas, N. L., Alivizatos, E. G., Kaklamani, D. I. & Anastassiu, H. T. (2007) Optimization of the method of auxiliary sources (MAS) for oblique incidence scattering by an infinite dielectric cylinder. *Electrical Engineering*, **89**(5), 353–361.

Wang, H. & Nakamura, G. (2012) The integral equation method for electromagnetic scattering problem at oblique incidence. *Applied Numerical Mathematics*, **62**(7), 860–873.

Wu, Y. & Lu, Y. Y. (2008) Dirichlet-to-Neumann map method for analyzing interpenetrating cylinder arrays in a triangular lattice. *Journal of the Optical Society of America B*, **25**(9), 1466–1473.